Brain Struct Funct (2016) 221:2375–2383
DOI 10.1007/s00429-015-1020-0

SHORT COMMUNICATION

Simplified CLARITY for visualizing immunofluorescence labeling in the developing rat brain

Huiyuan Zheng · Linda Rinaman

Received: 14 January 2015 / Accepted: 24 February 2015 / Published online: 14 March 2015

Abstract CLARITY is an innovative technological advance in which intact biological tissue is transformed into a "nanoporous hydrogel-hybridized form" (Chung et al. 2013; Chung and Deisseroth 2013) with markedly improved chemical and optical accessibility, permitting fluorescent visualization and extraction of high-resolution structural data from mm-thick blocks of tissue. CLARITY affords an excellent but as yet unexploited opportunity to visualize the growth and maturation of phenotypically identified neurons and axonal processes in the developing brain. This brief report describes a moderately revised, simplified, and less expensive CLARITY protocol that effectively reveals the structure of chemically identified neurons in whole neonatal/juvenile rat brains and tissue slabs. Rats [postnatal day (P)0–24] were transcardially perfused with one of two fixative/hydrogel solutions, followed by hydrogel polymerization to generate brain hybrids. Whole brain hybrids or 2.0-mm-thick coronal slabs were passively cleared of lipid and then processed for dual immunofluorescence labeling, including labeling using tyramide signal amplification. After refractive index matching using 2,20-Thiodiethanol (60 % solution), a Leica confocal microscope equipped with a CLARITY objective was used to view the hypothalamus in whole brain hybrids or slabs. Collected image stacks revealed the distribution and three-dimensional structure of hypothalamic pro-oxyphysin (oxytocin)-, neuropeptide Y-, glucagon-like peptide-1-, and tyrosine hydroxylase-immunopositive neurons and processes within large tissue volumes. Outstanding structural preservation and immunolabeling quality demonstrates the efficacy of this approach for interrogating chemically defined neural circuits as they develop in postnatal rodent brain.

Keywords CLARITY · Neonatal · Immunofluorescence

Introduction

CLARITY (Clear, Lipid-exchanged, Acrylamide-hybridized Rigid, Imaging/immunostaining compatible, Tissue hYdrogel) is an exciting, recently developed technology that transforms intact biological tissue into a hybrid form in which lipids are replaced with exogenous elements for increased accessibility and three-dimensional visualization of nucleotide and protein-based structures (Chung and Deisseroth 2013). In CLARITY, the brain and other body tissues are infiltrated with hydrogel monomers in formaldehyde-based fixative to facilitate biomolecule-hydrogel crosslinking (Tomer et al. 2014; Chung and Deisseroth 2013; Yang et al. 2014). Polymerization then stabilizes the hybrid tissue structure, and permits subsequent extraction of lipid molecules that otherwise limit tissue diffusion of primary antibodies, fluorescently conjugated secondary antibodies, complementary DNA and RNA strands, and other labeling probes. Importantly, the relative absence of lipid molecules in transformed tissue-hydrogel hybrids renders them optically clear ("see-through") and ideally suited for confocal imaging and three-dimensional analysis of fluorescent labeling patterns across continuous expanses of intact tissue.

Several published reports describe the successful use of CLARITY for analysis of fluorescent signals in formalin-fixed adult mouse brain and other tissues, including human brain (Chung and Deisseroth 2013; Chung et al. 2013; Yang

Electronic supplementary material The online version of this article (doi:10.1007/s00429-015-1020-0) contains supplementary material, which is available to authorized users.

H. Zheng · L. Rinaman (✉)
Department of Neuroscience, University of Pittsburgh, A210 Langley Hall, Pittsburgh, PA 15260, USA
e-mail: rinaman@pitt.edu

et al. 2014; Tomer et al. 2014). The original CLARITY procedure includes active extraction of lipids from transformed hybrid tissue using an electrophoretic tissue clearing (ETC) technique that accelerates the extraction process, but is technically complex and potentially damaging to fragile tissues (such as embryonic or neonatal rat brains). A passive tissue clearing approach using different fixative-hydrogel monomer crosslinking solutions was subsequently introduced to hybridize tissues obtained from adult rodents or human postmortem brain (Tomer et al. 2014; Yang et al. 2014), but its efficacy has not been tested in the particularly fragile brain tissue of neonatal rats, and fluorescent immunolabeling procedures that include amplification/enhancement of signals for sparse antigens have not been reported. Further, the potential utility of including acrolein (the simplest unsaturated aldehyde) as a component of the hydrogel-aldehyde fixative solution to improve the structural integrity of fragile tissues (such as neonatal rat brain) is unreported.

Given our laboratory's research interest in the pre- and postnatal development of central brainstem/hypothalamic/limbic forebrain circuits, we sought to develop an inexpensive, simplified passive CLARITY protocol that would be broadly applicable for immunocytochemical analyses of the developing rat brain. Two hydrogel-aldehyde fixation solutions, a simplified polymerization step, an amplified immunofluorescence labeling protocol, and an alternative clearing and storage protocol for refractive index matching (RIM) were tested to optimize both structural tissue integrity and confocal visualization of sparse or weakly expressed neurotransmitter-related epitopes. This report details our successful protocol, to assist others seeking to apply the promising technological innovation offered by CLARITY to their own scientific questions.

Materials and methods

Animals

Experimental protocols were approved by the University of Pittsburgh Institutional Animal Care and Use Committee. The male and female progeny of 2 pregnant multiparous Sprague-Dawley rats (Harlan Laboratories, Indianapolis, IN, USA) were used in this study. Pregnant rats arrived at a gestational stage between embryonic days 17 and 18 and were housed singly in polyethylene cages in a controlled environment (20–22 °C; 12:12 h light:dark cycle), with ad libitum access to water and pelleted rat chow (Purina #5001, Bethlehem, PA, USA). Pregnant rats were checked daily to determine their pups' date of birth, designated postnatal day (P)0. Pup sex was determined by measuring anogenital distance (Jackson 1912).

Solutions

The commercial sources of reagents referred to below are provided in Table 1. Mixtures and working concentrations are as follows:

1. Hydrogel solution A: Paraformaldehyde (PF)-acrylamide
   - 1X phosphate-buffered saline solution (PBS, pH 7.4; prepared by diluting 10X PBS 1:10 in dH_20) containing 4.0 % PF (vol/vol), 4.0 % acrylamide (vol/vol), and 0.25 % VA-044 initiator (wt/vol) (Note: bisacrylamide is not used). Briefly, PF, acrylamide and VA-044 were stirred into 1X PBS at room temperature to dissolve, then immediately chilled on ice and kept cold until used for transcardiac perfusion, within 1–2 h. Additional solution (30 ml/brain) was reserved for postfixation and hydrogel polymerization.
2. Alternative Hydrogel solution B: Acrolein-PF-acrylamide
   - 1X PBS containing 2.0 % PF (vol/vol), 4.0 % acrylamide (vol/vol), and 0.25 % VA-044 initiator (wt/vol) was prepared as for solution A, above, and kept cold until used for perfusion within 1–2 h. Additional solution (30 ml/brain) was reserved for postfixation and hydrogel polymerization. Acrolein (2.0 % final concentration, vol/vol) was added to

Table 1 Reagents and commercial sources

Reagent	Source, product #
40 % Acrylamide solution	Bio-Rad, 161-0140
10X Phosphate-buffered saline, pH 7.4	Invitrogen, GIBCO 10010
2,2′-Azobis[2-(2-imidazolin-2-yl) propane] dihydrochloride (VA-044 initiator)	Wako, 27776-21-2
Paraformaldehyde aqueous solution, 16 %	Electron Microscopy Sciences, 15710-S
Boric acid	Sigma–Aldrich, B3637
Sodium dodecyl sulphate (SDS)	Promega, H5114
2,20-Thiodiethanol	Sigma–Aldrich, 166782
Acrolein	Polysciences, 00016

the perfusion solution just before perfusion (Note: acrolein was excluded from the postfixation and hydrogel polymerization solution).

3. Tissue clearing solution (Chung et al. 2013):
   - 0.2 M boric acid (pH 8.5) containing 4.0 % sodium dodecyl sulphate (SDS).
4. Rinsing buffer for immunofluorescent labeling (IFL):
   - 0.5 M boric acid (pH 8.5) containing 0.1 % triton-X100.
5. Antibody diluent for IFL:
   - 0.5 M boric acid containing 0.1 % triton-X100 and 1.0 % normal donkey serum.
6. Refractive index matching (RIM) medium:
   - 2,20-Thiodiethanol (TDE) diluted to concentrations of 20, 40 and 60 % in 1X PBS.

Transcardiac perfusion, brain postfixation and hybridization, and hybrid tissue clearing

Rat pups were deeply anesthetized with pentobarbital sodium (130 mg/kg, i.p., Fatal Plus Solution; Butler Schein), then transcardially perfused with 10 ml (P0, P4) or 20 ml (P17, P24) of ice-cold 1X PBS, followed by 30 ml (P0, P4) or 150 ml (P17, P24) of ice-cold hydrogel solution A or B. When solution B was used, an additional 25–100 ml (depending on pup age) of PF (2 %)-hydrogel solution (without acrolein) was subsequently perfused to remove acrolein from fixed tissues before handling. Fixed brains were immediately extracted from the skull, placed individually into 50 ml Falcon conical tubes containing 30 ml of hydrogel postfixation solution, and stored overnight at 4 °C. To minimize exposure of hydrogel-immersed brain hybrids to oxygen in the air, a 4- to 5-mm-thick layer of mineral oil was gently laid over the top of the hydrogel solution before the tubes were tightly capped. This eliminated the need for nitrogen degassing, described by others as necessary for subsequent polymerization of acrylamide monomers (Chung et al. 2013; Yang et al. 2014). Polymerization was carried out for 3 h in a 37 °C water bath without shaking.

After polymerization, a subset of hybridized P17 and P24 brains were blocked coronally through the level of the midbrain (i.e., at the rostral extent of the cerebellum) into forebrain and brainstem components. The cerebellum was discarded after it was separated from the brainstem by severing the cerebellar peduncles bilaterally. The forebrain was cut coronally into 2.0-mm-thick slabs using a tissue mold. Remaining whole brains (P0, P4, P17, P24), brainstems, and coronal forebrain slabs (P17, P24) were submerged in 40 ml of tissue clearing solution in 50 ml Falcon conical tubes (one tube per rat), tightly capped, and placed on a rotating platform (Maxi Mix III, Barnstead International) in a 37 °C incubator (VWR Shelf-1545; 100 rotations/min) to enable passive tissue clearing. Tissue clearing solution was replaced with 40 ml of fresh solution each day for the first week. Some samples were clear within a week, whereas others required additional time (see Table 2). For the latter, tissue clearing solution was replaced three times a week until tissues were visibly cleared. Cleared whole brains, brainstems, and coronal slabs were either processed for IFL immediately, as described below, or were stored in tissue clearing solution for up to 9 months at room temperature for later initiation of IFL procedures (e.g., Fig. 4).

Table 2 Passive clearing times

Tissue	Age	Days
Whole brain	P0	6–8
Whole brain	P4	10–12
Whole brain	P17	20–25
Whole brain	P24	30–40
Brainstem block	P17	20–25
Brainstem block	P24	30–40
2.0-mm brain slabs	P17	12–15
2.0-mm brain slabs	P24	16–20

Immunofluorescence labeling (IFL)

Cleared tissue samples were transferred into 20 ml glass scintillation vials for IFL. All antibody incubations and rinses were conducted on a rotating platform in a 37 °C incubator. Table 3 summarizes the primary and secondary antibodies included in the current report, and their working dilutions (in antibody diluent). Each "rinse" was conducted over 24 h in four changes of rinsing buffer, unless noted otherwise.

First, hybrid tissues were rinsed to remove residual SDS. A cocktail of two primary antibodies raised in different species (Table 3) recognizing neuropeptide Y (NPY), pro-oxyphysin [expressed by immature and mature oxytocin (OT) neurons; (Rinaman 1998)] and/or tyrosine hydroxylase (TH) was used to achieve dual IFL of these robustly expressed antigens. Briefly, hybrid tissues were incubated in primary antibody cocktail for 72 h, rinsed, and then incubated for 48 h in a cocktail of the corresponding species-specific secondary antibodies conjugated to distinct fluorescent tags (Table 3), followed by a final rinse.

Glucagon-like peptide (GLP-1) IFL within the rat brain is significantly more sparse compared to NPY, pro-

Table 3 Immunofluorescence reagents

Reagent	Dilution	Source, product number
Rabbit anti-glucagon-like peptide-1	1:1500	Peninsula Laboratories, T-4363
Sheep anti-neuropeptide Y	1:500	Millipore, AB1583
Mouse anti-pro-oxyphysin (PS38)	1:200	ATCC (hybridoma cells), CRL-1950
Mouse anti-tyrosine hydroxylase	1:500	Millipore, MAB318
Alexa 647-conjugated donkey anti-sheep IgG	1:300	Jackson ImmunoResearch, 713-605-003
Alexa 647-conjugated donkey anti-mouse IgG	1:300	Jackson ImmunoResearch, 715-606-151
Cyanine 3-conjugated donkey anti-mouse IgG	1:300	Jackson ImmunoResearch, 715-165-150
Cyanine 3-conjugated tyramide	1:250	PerkinElmer, SAT704B001
Horseradish peroxidase-conjugated donkey anti-rabbit IgG	1:400	Millipore, AP182P
Normal donkey serum		Jackson ImmunoResearch, 017-000-121

oxyphysin, or TH. To visualize GLP-1 IFL in hybrid brain tissue, labeling was enhanced using tyramide signal amplification, as recently reported for rat brain tissue processed using standard histological techniques (Zheng et al. 2014). Hybrid tissues were incubated in a cocktail of pro-oxyphysin and GLP1 primary antibodies for 72 h, rinsed, and then incubated for 48 h in a cocktail of Alexa647-conjugated donkey anti-mouse IgG and horseradish peroxidase (HRP)-conjugated donkey anti-rabbit IgG. Tissues were rinsed for a total of 5–8 h using 4–5 changes of rinsing buffer, reacted for 3–5 h in Cyanine 3 (Cy3)-conjugated tyramide, and then given a final rinse.

Refractive index matching (RIM)

RIM was conducted at room temperature without shaking. After completing IFL, tissue hybrids were equilibrated in 1X PBS overnight at room temperature before transitioning into TDE solutions at progressively higher concentrations. RIM was achieved by sequentially submerging tissue hybrids in 20 %, 40 %, 60 % TDE solution for 4–12 h each. The time in each solution varied depending on tissue volume, and hybrid tissues were transitioned from one solution to the next after sinking in the former. Hybrid tissues were then passed through three changes of fresh 60 % TDE over 24 h. After RIM, hybrid tissues were stored in 60 % TDE solution at room temperature for later imaging of IFL. The 60 % concentration of TDE has a refractive index of 1.45 (Staudt et al. 2007), matching the refractive index of clarified brain tissue (Chung et al. 2013) and the Leica CLARITY objective used for imaging, below.

Imaging

Images were acquired using a Leica TCS SP8 confocal microscope equipped with a 25X CLARITY objective (6.0-mm working distance; HC FLUOTAR L 25×/1.00 IMM; ne = 1.457; motCORR VISIR; Leica) designed to match the 1.45 refractive index of clarified tissue hybrids (microscope access provided by Dr. Jianxin Bao, Northeastern Ohio Medical University, Rootstown, OH). At the time of imaging, hybrid tissues were transferred into fresh 60 % TDE solution contained within a black-walled, glass-bottomed Willco Dish (Ted Pella, 14032-120). A putty rim (Scotch Removable Mounting Putty, St. Paul, MN) was built up manually inside the walls of the dish to form a deeper pool of TDE that covered the hybrid tissue sample. The CLARITY objective was then dipped directly into TDE solution to bring IFL within the desired region of the sample into focus, with no coverslip intervening between the hybrid tissue and the objective lens (see Fig. 2a). The Cy3 fluorophore was excited using a 552 nm OPSL laser, and Alexa 647 was excited using a 638 nm Diode laser. Images were collected using Leica LAS 4.0 image collection software, and using the 3D Visualization module for rendering/reconstructing tissue volumes and for making "movies" in which the 3D volumes are zoomed in and out and rotated (see supplementary Video). Additional details regarding image collection are included in the figure legends.

Results

Passive clearing of hybrid tissue

The passive tissue clearing method was well suited for whole rat brains from P0 to P24, and also for 2.0-mm-thick tissue slabs (P17 and P24). Figure 1 depicts a clarified whole brain hybrid from a newborn (P0) pup perfused with Hydrogel solution A, and a 2.0-mm-thick coronal slab containing the hypothalamus from a juvenile (P24) rat

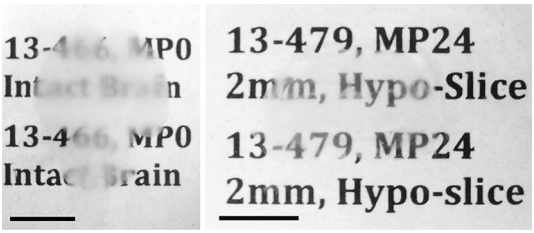

Fig. 1 Representative low-magnification photographs of clarified brain hybrids. *Left* intact (whole) brain hybrid from a newborn male rat pup (P0) perfused with Hydrogel solution A. *Right* 2-mm-thick hybrid tissue coronal slab through the level of the hypothalamus in a juvenile male rat (P24) perfused with Hydrogel solution B. *Scale bars* 500 μm

perfused with Hydrogel solution B. The time required for clearing hybrid tissues increased with postnatal age and thickness of the hybrid sample (Table 2), but was consistent for each sample type. As previously reported (Chung et al. 2013; Yang et al. 2014), the volume of tissue hybrids increased noticeably during the clearing process but normalized after completion of RIM. For example, after RIM, the thickness (2 mm), width (14.1 mm), and height (10.2 mm) of a representative hybrid tissue slab from a P24 rat perfused with hydrogel Solution B matched measurements obtained from the same sample before clearing. Further, the dorsal–ventral and medial–lateral measurements of the sample after RIM were similar to those provided for a coronal section through the level of the hypothalamus in a standard adult rat brain stereotaxic atlas (Swanson 2004).

TDE for refractive index matching and storage of IF-labeled hybrid tissues

With a stepwise transition of IFL-processed hybrid tissues from rinsing buffer into TDE solutions of increasing concentration, the tissues became progressively clearer over a 24–36 h period, depending on tissue volume. IFL using secondary antibodies conjugated to Cy3, Alexa-647 or DAPI (not shown) were well preserved after storage of labeled tissues in 60 % TDE solution at room temperature for up to 9 months (e.g., Fig. 3).

Dual IFL in intact, whole brain hybrids

Figure 2 illustrates dual IFL for TH and NPY within the medial hypothalamus (image z-stack = 591 μm) in an intact brain hybrid from a newborn (P0) pup perfused with hydrogel solution A. The depicted z-stack image (Fig. 2a) was captured with the ventral surface of the diencephalon positioned beneath the 25X CLARITY objective. The inset in Fig. 2a is a photograph of this specific intact brain hybrid obtained during the confocal imaging session. TH-positive cell bodies and processes (green) of dopaminergic hypothalamic neurons (A12/A13 cell groups) are visible bilaterally on each side of the 3rd ventricle. A sparser population of NPY-positive profiles (red) also is visible. Figure 2b depicts a 3D rendering of the same hypothalamic volume (0.137 mm^3; 393 μm × 591 μm × 591 μm; see also supplementary video), rotated to reveal that medial hypothalamic NPY labeling in the newborn rat brain is most dense near the ventral surface (i.e., Z range from 0 to 150 μm, top of Fig. 2b).

Dual IFL in 2.0-mm-thick slabs

Figure 3 depicts dual pro-oxyphysin (OT; green) and NPY (red) IFL in a 2.0-mm-thick coronal tissue slab through the anterior medial hypothalamus of a P24 male rat (image z-stack in Fig. 3a = 252 μm). This animal was perfused with the alternative hydrogel solution B, containing 2 % acrolein. Addition of acrolein to the fixative solution led to tissue hybrids that were firmer but exhibited a pale amber color that was maintained after clearing. However, the pale amber coloration did not impede confocal imaging of IFL within the tissue, and was actually useful during tissue handling and orientation. The medial surface of the anterior paraventricular nucleus of the hypothalamus (PVN; i.e., adjacent to the 3rd ventricle) is positioned to the right of the image (Fig. 3a). Close inspection of the rotated volume from all angles indicated that NPY-positive terminals occupy the spaces between OT-positive neurons, but do not appear to form close appositions with OT-positive perikaryal surfaces.

Tyramide-enhanced IFL in 2.0-mm-thick slabs

Figure 4 illustrates dual IFL of pro-oxyphysin (OT; green) and GLP-1 (red) in a 2.0-mm-thick coronal slab of tissue through the hypothalamus of a P24 rat (image z-stack = 536 μm) perfused with the acrolein-containing hydrogel solution B. Tyramide signal amplification was used to enhance what is otherwise a relatively sparse GLP-1 IFL signal. This procedure revealed a dense GLP-1-positive terminal field within the posterior paraventricular nucleus of the hypothalamus (PVN), as previously reported in 35 μm-thick tissue sections from adult rats prepared using standard histological methods and tyramide-enhanced immunolabeling (Zheng et al. 2014).

Discussion

The present short report documents the effectiveness of a moderately revised passive CLARITY protocol for

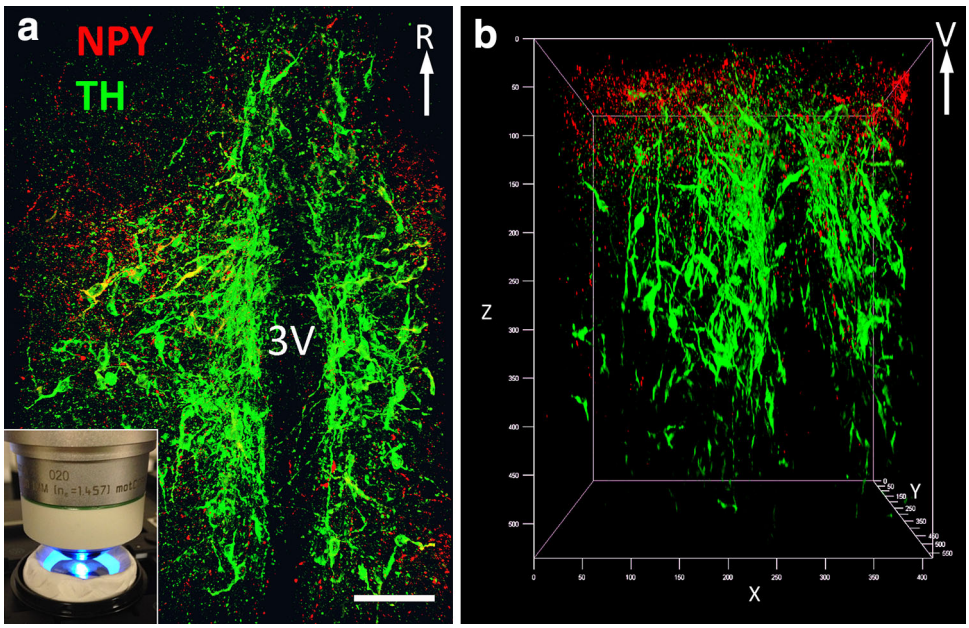

Fig. 2 Dual IFL for NPY (Alexa-647, imaged in *red channel*) and TH (Cy3, imaged in *green channel*) within the medial hypothalamus of a clarified intact (whole) brain hybrid prepared from a newborn rat pup (P0) perfused with Hydrogel solution A. **a** Maximum intensity flattened Z-projection obtained from 262 1.5 μm-thick optical frames (393 μm). This confocal image was obtained using a ventral approach. The total volume of the flattened image is 0.137 mm^3 (i.e., 591 μm × 591 μm × 393 μm). The *inset* in **a** is a photograph of this hybrid sample, positioned ventral side up, that was obtained during confocal image collection. **b** Rotated view of the z-stack depicted in **a** (ventral is at the *top*, *V*). See the supplementary video for a 3D rendering of the entire volume. *Scale bar* in **a** 100 μm. *3V* third ventricle; *R* rostral (color figure online)

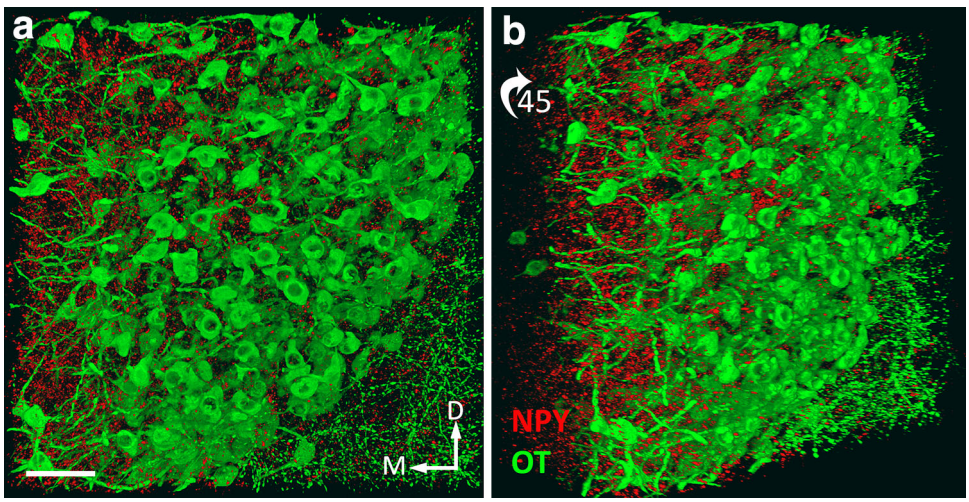

Fig. 3 Dual IFL of OT (Cy3, imaged in *green channel*) and NPY (Alexa-647, imaged in *red channel*) in a 2.0-mm-thick coronal slab through the level of the diencephalon in a juvenile male rat (P24) perfused with Hydrogel solution B. **a** A maximum intensity Z-projection obtained from 428 0.59 μm optical sections (i.e., 252 μm). The total image volume is 0.032 mm^3 (i.e., 354 μm × 354 μm × 252 μm). **b** A 45° clockwise rotation of the z-stack shown in **a**. *Scale bar* 100 μm. See supplementary video for a 3D rendering and rotation of the entire volume (color figure online)

interrogating chemically distinct neural populations in fragile, developing rat brain tissue. The goal of our work was to develop a simplified, less expensive, accessible, and widely applicable CLARITY protocol to obtain high-resolution, three-dimensional images of immunofluorescent labeling in developing rat brain. Application of the procedures described in this report generated rat brain hybrids with outstanding structural preservation and immunolabeling quality, demonstrating the utility of this passive CLARITY protocol for visualizing chemically defined neural systems in fragile tissue samples. For the antibodies tested, immunofluorescent labeling quality in

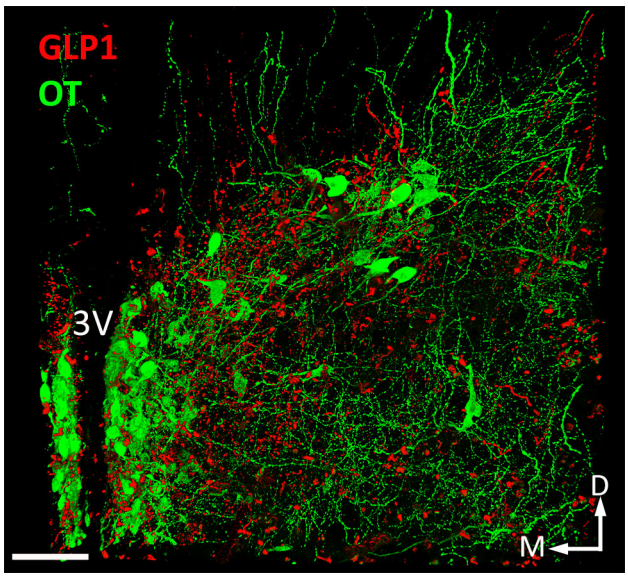

Fig. 4 Dual IFL for OT (Alexa-647, imaged in *green channel*) and GLP1 (TSA-Cy3, imaged in *red channel*) in a 2.0-mm-thick coronal slab through the diencephalon in a juvenile male rat (P24) perfused with Hydrogel solution B. This image is a maximum intensity Z-projection obtained from 268 2.0 µm optical sections (i.e., 536 µm thick). The total image volume is 0.127 mm^3 (i.e., 410 µm × 579 µm × 536 µm). *3V* third ventricle, *D* dorsal, *M* medial. *Scale bar* 100 µm (color figure online)

clarified tissue (whole brains and 2-mm-thick slabs) is as good or better than labeling achieved in standard thin-sectioned brain tissue (Maniscalco and Rinaman 2013; Kreisler et al. 2014; Zheng et al. 2014; Rocha et al. 2014; Taksande et al. 2011; Grove and Smith 2003; Rinaman 1998), validating the superior antigen preservation properties of the CLARITY technique (Chung and Deisseroth 2013; Chung et al. 2013).

Compared to the first detailed published CLARITY protocol (Chung et al. 2013), the principle modifications and extensions of the protocol described in the present report include the following:

Transcardiac perfusion with a new acrylamide-paraformaldehyde-acrolein crosslinking solution

Addition of acrolein to the hydrogel-paraformaldehyde solution increased the rigidity of neonatal rat brain hybrids, with no apparent compromise in subsequent lipid clearing, immunofluorescent labeling, or optical accessibility during imaging. The rationale for including acrolein in the hydrogel perfusing solution was based on prior work in our laboratory and others indicating that acrolein use significantly improves tissue structure and immunolabeling signal-to-noise ratio in light and electron microscopic studies (Rinaman 1999; Balcita-Pedicino and Rinaman 2007; Koehnle and Rinaman 2007). In the present study, inclusion of acrolein generated brain hybrids with a pale amber coloration, which facilitated tissue handling and orientation during immunoprocessing and confocal imaging. The coloration did not appear to impede or scatter light, and thus, did not interfere with confocal imaging. It should be noted, however, that acrolein is highly toxic (see Material Safety Data Sheet, available online): solution preparation and animal perfusion must be conducted in a laboratory ventilation hood that is approved for the use of volatile, toxic materials. Unused acrolein and solutions containing acrolein should be inactivated (biodegraded) by exposure to an excess volume of 2 % sodium bisulfite. In the present protocol, acrolein is used during animal perfusion only, and is excluded from the postfixation and hydrogel polymerization solutions.

Omission of nitrogen de-gassing before hydrogel polymerization

The addition of a thin layer of mineral oil over the top of the hydrogel solution before polymerization of brain hybrids eliminated the need for nitrogen degassing, described by others as necessary for acrylamide monomer polymerization (Chung et al. 2013; Yang et al. 2014). The oil layer effectively separated hybrid tissues from oxygen in the air (which impedes hydrogel polymerization), simplifying the process and eliminating the need for a desiccation chamber, vacuum pump, and nitrogen tank.

Passive tissue clearing in ionic detergent solution

The passive clearing technique removes lipids without the harsh conditions of active-transport electrophoresis that can damage fragile tissue, and obviates the need for expensive ETC equipment. Although the first detailed published CLARITY protocol indicated that ETC was crucial for tissue preparation (Chung et al. 2013), we (present report) and others (Tomer et al. 2014) have found that the passive clearing protocol generates full transparency of hybrid tissues and excellent immunofluorescent labeling results. Indeed, the laboratory that developed the CLARITY technique states the following: "Whenever allowed by speed, tissue properties and other constraints, we advise passive thermal clearing rather than ETC" (Tomer et al. 2014). In an effort to speed up the passive clearing process in the present study, bisacrylamide was successfully omitted from the hydrogel monomer solution, which contained only 4 % acrylamide (in addition to aldehyde fixative). Another laboratory also has successfully omitted bisacrylamide from their hydrogel solution (Yang et al.

2014), although their solution lacked an aldehyde fixative. Thus, a variety of hydrogel solutions (i.e., with and without bisacrylamide, and with and without aldehyde fixative) have been used successfully for different tissue types and applications. As shown in Table 2, hybrid tissues cleared passively within 1–6 weeks, depending on sample volume. For a given preparation type and age (i.e., whole brain vs. 2-mm-thick slabs, P0 vs. P24), clearing times were consistent regardless of whether Hydrogel solution A or B was used.

The original CLARITY protocol was reported to produce a protein loss of approximately 8 % after ETC, significantly lower than protein loss using standard histological and immunocytochemical processing techniques. The absence of ETC in passive CLARITY may produce even less protein loss even when bisacrylamide is omitted from the hydrogel solution [e.g. (Yang et al. 2014)], and thus yield stronger immunofluoresence signals identifying sparse antigens (e.g., GLP-1 in the developing rat hypothalamus). Although protein loss was not quantified in the present study, the high quality immunolabeling that was achieved (i.e., high signal, low background) suggests a low level of protein loss, similar to that documented in a recent report (Yang et al. 2014).

Use of tyramide signal enhancement to boost immunofluorescence labeling of sparse antigens in clarified hybrid tissue

Because tyramide signal amplification can enhance what is otherwise a relatively sparse IFL signal, this procedure was applied to clarified hybrid tissues to localize GLP-1-positive fibers and terminals within the juvenile rat hypothalamus. The procedure described herein successfully revealed a dense GLP-1-positive terminal field within the PVN of 24-day-old rat brain hybrids. Indeed, GLP-1 immunolabeling quality in the present report (Fig. 3) was as good or better than labeling obtained in 35 µm-thick tissue sections from adult rats prepared using standard histological methods and tyramide-enhanced immunolabeling (Zheng et al. 2014). This approach will be used in future work to produce IFL for GLP-1 and other sparse antigens in brain hybrid tissue from younger rat pups, to document the pre- and postnatal structural development of axonal projections from chemically identified neurons in intact brain hybrids. This should yield significant advantages over our previous standard histological, brain sectioning, and immunocytochemical labeling approach investigating the structural development of brainstem-hypothalamic circuits [e.g. (Rinaman and Levitt 1993; Rinaman 1998, 2001)].

Use of 2,20-Thiodiethanol (TDE) for refractive index matching and tissue storage

Previously published CLARITY reports have used FocusClear to increase the transparency of tissue samples, and for RIM during fluorescent image collection (Chung and Deisseroth 2013; Chung et al. 2013). The present results suggest that 60 % TDE is equally effective for RIM and hybrid tissue storage after IFL. There is a clear economic advantage to using TDE: the current cost of a 60 % solution of TDE solution is more than 700 times less than the cost of an equivalent working volume of FocusClear, and more than 60 times less expensive than an equivalent working volume of an alternative Histodenz-based solution used in another recent report (Yang et al. 2014). TDE is non-toxic and water miscible in any concentration, and its refractive index depends on its concentration (Staudt et al. 2007). Further, the antioxidant and reducing properties of TDE preserve the fluorescence quantum yield of most fluorophores (Staudt et al. 2007), help to attenuate photobleaching of fluorescent signals during imaging, and permit long-term preservation of clarified/IF-labeled tissue. However, to obtain complete optical clearing and RIM, it is important that a slow stepwise transition from rinsing buffer to ascending TDE solutions be used to allow equilibrium in each solution.

Direct dipping of the CLARITY microscope objective into TDE during imaging

During confocal imaging of material generated in the present report, the 25X CLARITY microscope objective (Leica) was dipped directly into 60 % TDE solution, with no coverglass intervening between the objective lens and the hybrid tissue sample. Leica has confirmed that such contact is safe, and will not damage the objective. This obviates the need to "sandwich and seal" the hybrid tissue between two glass surfaces [as described in (Chung et al. 2013)], and removes another source of light scattering and image distortion during data collection. However, it is important to ensure that the hybrid tissue does not move during imaging. In the present report, images were collected over a relatively brief time period (~2–3 h), and only from the tissue area located directly below the microscope objective (i.e., the samples were not moved during imaging). In future work in which longer periods of image collection from multiple regions of the sample are conducted, fine nylon threads or mesh may be necessary to gently secure samples to the bottom of the TDE-filled glass dish.

Conclusion and future directions

Outstanding structural preservation and immunolabeling quality demonstrates the efficacy of the modified CLARITY approach described in this report for interrogating chemically defined neural circuits as they develop in postnatal rodent brain. By facilitating anatomical identification of chemically defined neurons and processes, including axonal projections traversing long distances within unsectioned tissue, CLARITY offers an improved opportunity for our laboratory and others to relate progressive structural events in circuit maturation to the functional emergence of complex neural systems and the functionalities they support [e.g. (Bouret et al. 2004; Koehnle and Rinaman 2007; Rinaman 2001, 2003)]. However, and as pointed out by the researchers who originally developed CLARITY (Chung et al. 2013), a remaining challenge (and the next step for our own work) will be optimization of computerized protocols for collecting, manipulating, and integrating immense sets of imaging data obtained from larger continuous brain regions, to visualize and analyze the structural development of large-scale intact neural circuits.

References

Balcita-Pedicino JJ, Rinaman L (2007) Noradrenergic axon terminals contact gastric pre-autonomic neurons in the paraventricular nucleus of the hypothalamus in rats. J Comp Neurol 501:608–618

Bouret SG, Draper SJ, Simerly RB (2004) Formation of projection pathways from the arcuate nucleus of the hypothalamus to hypothalamic regions implicated in the neural control of feeding behavior in mice. J Neurosci 24:2797–2805

Chung K, Deisseroth K (2013) CLARITY for mapping the nervous system. Nat Methods 10(6):508–513. doi:10.1038/nmeth.2481

Chung K, Wallace J, Kim SY, Kalyanasundaram S, Andalman AS, Davidson TJ, Mirzabekov JJ, Zalocusky KA, Mattis J, Denisin AK, Pak S, Bernstein H, Ramakrishnan C, Grosenick L, Gradinaru V, Deisseroth K (2013) Structural and molecular interrogation of intact biological systems. Nature 497(7449): 332–337. doi:10.1038/nature12107

Grove KL, Smith MS (2003) Ontogeny of the hypothalamic neuropeptide Y system. Physiol Behav 79(1):47–63

Jackson CM (1912) On the recognition of sex through external characters in the young rat. Biol Bull 23(3):171–173

Koehnle T, Rinaman L (2007) Progressive postnatal increases in Fos immunoreactivity in the forebrain and brainstem of rats after viscerosensory stimulation with lithium chloride. Am J Physiol Regul Integr Comp Physiol 292:R1212–R1223. doi:10.1152/ajpregu.00666.2006

Kreisler AD, Davis EA, Rinaman L (2014) Differential activation of chemically identified neurons in the caudal nucleus of the solitary tract in non-entrained rats after intake of satiating vs. non-satiating meals. Physiol Behav 136:47–54. doi:10.1016/j.physbeh.2014.01.015

Maniscalco JW, Rinaman L (2013) Overnight food deprivation markedly attenuates hindbrain noradrenergic, glucagon-like peptide-1, and hypothalamic neural responses to exogenous cholecystokinin in male rats. Physiol Behav 121:35–42. doi:10.1016/j.physbeh.2013.01.012

Rinaman L (1998) Oxytocinergic inputs to the nucleus of the solitary tract and dorsal motor nucleus of the vagus in neonatal rats. J Comp Neurol 399(1):101–109

Rinaman L (1999) Interoceptive stress activates glucagon-like peptide-1 neurons that project to the hypothalamus. Am J Physiol Regul Integr Comp Physiol 46)277:R582-R590

Rinaman L (2001) Postnatal development of catecholamine inputs to the paraventricular nucleus of the hypothalamus in rats. J Comp Neurol 438:411–422

Rinaman L (2003) Postnatal development of hypothalamic inputs to the dorsal vagal complex in rats. Physiol Behav 79:65–70

Rinaman L, Levitt P (1993) Establishment of vagal sensorimotor circuits during fetal development in rats. J Neurobiol 24(5):641–659

Rocha ML, Fernandes PP, Lotufo BM, Manhaes AC, Barradas PC, Tenorio F (2014) Undernutrition during early life alters neuropeptide Y distribution along the arcuate/paraventricular pathway. Neuroscience 256:379–391. doi:10.1016/j.neuroscience.2013.10.040

Staudt T, Lang MC, Medda R, Engelhardt J, Hell SW (2007) 2,2′-Thiodiethanol: a new water soluble mounting medium for high resolution optical microscopy. Microsc Res Tech 70(1):1–9. doi:10.1002/jemt.20396

Swanson L (2004) Brain maps III. Structure of the rat brain. Elsevier, Amsterdam

Taksande BG, Kotagale NR, Nakhate KT, Mali PD, Kokare DM, Hirani K, Subhedar NK, Chopde CT, Ugale RR (2011) Agmatine in the hypothalamic paraventricular nucleus stimulates feeding in rats: involvement of neuropeptide Y. Br J Pharmacol 164(2b):704–718. doi:10.1111/j.1476-5381.2011.01484.x

Tomer R, Ye L, Hsueh B, Deisseroth K (2014) Advanced CLARITY for rapid and high-resolution imaging of intact tissues. Nat Protoc 9(7):1682–1697. doi:10.1038/nprot.2014.123

Yang B, Treweek JB, Kulkarni RP, Deverman BE, Chen CK, Lubeck E, Shah S, Cai L, Gradinaru V (2014) Single-cell phenotyping within transparent intact tissue through whole-body clearing. Cell 158(4):945–958. doi:10.1016/j.cell.2014.07.017

Zheng H, Stornetta RL, Agassandian K, Rinaman L (2014) Glutamatergic phenotype of glucagon-like peptide 1 neurons in the caudal nucleus of the solitary tract in rats. Brain Struct Funct. doi:10.1007/s00429-014-0841-6